Optical and gamma-ray variability in blazars

Gopal Bhatta
Institute of Nuclear physics, PAN
Krakow, Poland

The Variable Multi-Messenger Sky
Polish-German WE-Heraeus-Seminar
07 - 10 November 2022
Krakow, Poland

What are Blazars?

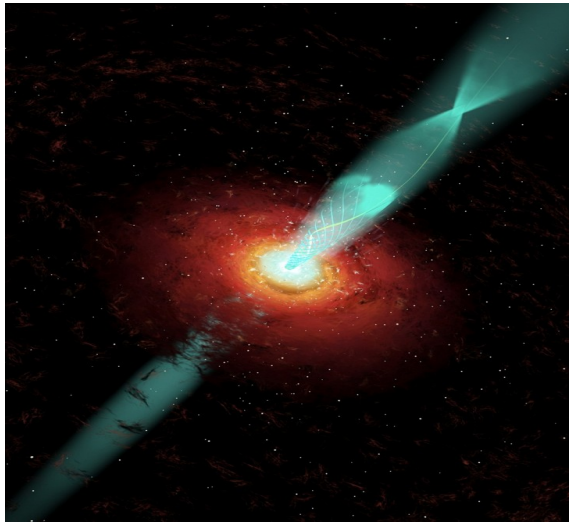

Observational properties:

- high amplitude, rapid variability,
- high optical and radio polarization,
- broadband non-thermal SED is highly Doppler boosted
- Dominant gamma-ray emission

Doppler Factor $\delta = 1/[\Gamma(1-\beta\cos\theta)]$

$$\nu = \nu'\,\delta$$

$$I(\nu) = \delta^3 I'(\nu')$$

- Blazars are a small subset of active galactic nuclei (AGN), powered by central black hole and ejecting relativistic jets

Blazar Multi-wavelength variability

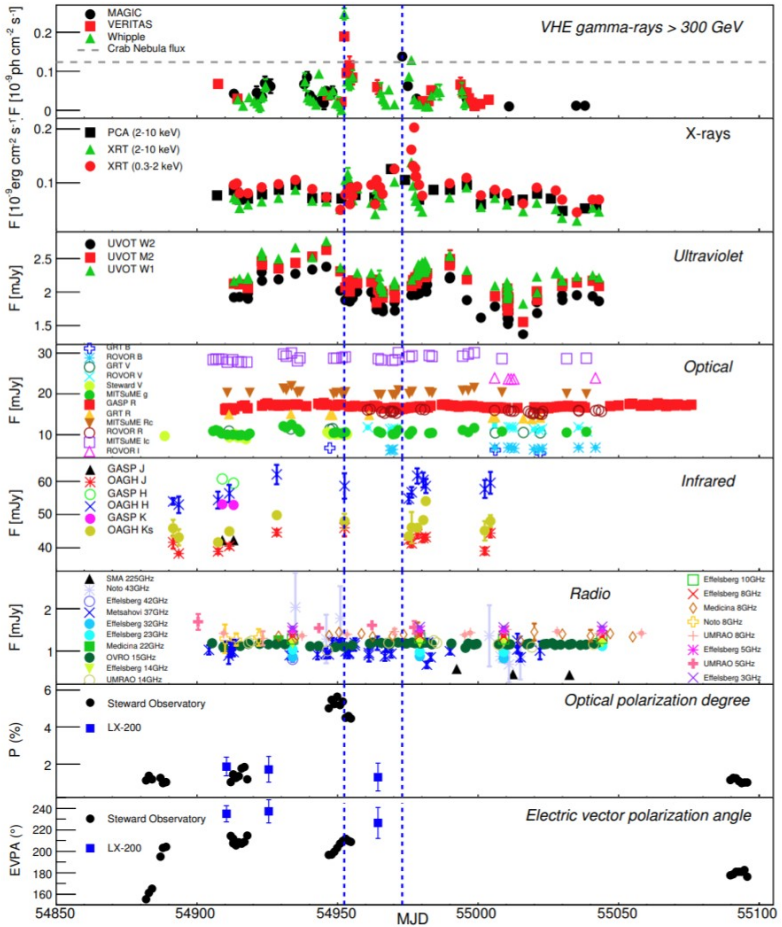

Mrk 501 from Ahnen et. al 2007

As in many case, the sources are not resolved in any of the current instruments the MWL variability studies become of the of the most power tools to explore the sources.

Motivation: multimessenger approach

- It is noted that the energy density of cosmic neutrinos with an that matches that of the cosmic high-energy photons and UHECRs,
- This suggests that neutrinos, gamma-ray and high-energy cosmic rays share a common origin.
- RL AGN or blazars can be promising candidate sources contributing to MMS emission.
- It becomes important to study the dynamics of AGN central engines

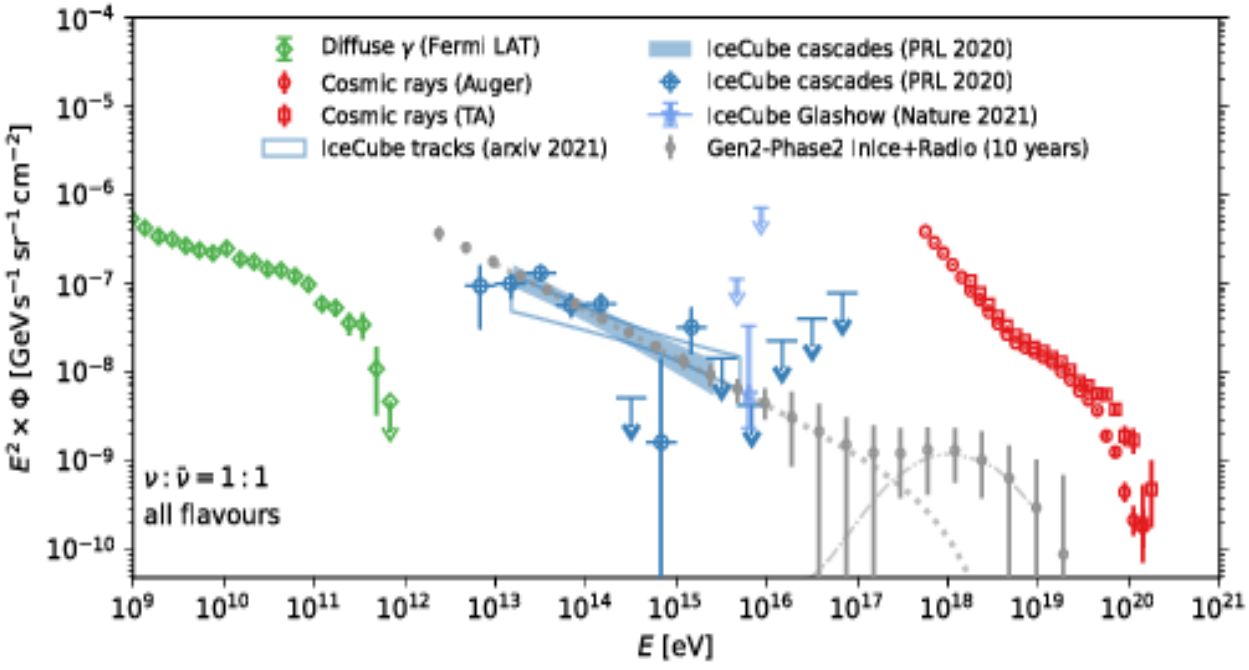

Sample sources

Fractional variability

$$F_{\rm var} = \sqrt{\frac{S^2 - \langle \sigma_{\rm err}^2 \rangle}{\langle F \rangle^2}}$$

The Astrophysical Journal, 891:120 (25pp), 2020 March 10

Table 1
Source Sample of the *Fermi*/LAT Blazars

Source Name (1)	3FGL Name (2)	Source Class (3)	R.A. (J2000) (4)	Decl. (J2000) (5)	Redshift (6)	FV (%) (7)	$\beta \pm \Delta\beta$ (8)
3C 66A	3FGL J0222.6+4301	BL Lac	$02^h22^m41^s.6$	$+43^d02^m35^s.5$	0.444	58.43 ± 1.78	0.90 ± 0.17
AO 0235+164	3FGL J0238.6+1636	BL Lac	$02^h38^m38^s.9$	$+16^d36^m59^s$	0.94	95.53 ± 1.12	1.40 ± 0.19
PKS 0454−234	3FGLJ0457.0-2324	BL Lac	$04^h57^m03^s.2$	$-23^d24^m52^s$	1.003	68.25 ± 1.06	1.10 ± 0.09
S5 0716+714	3FGL J0721.9+7120	BL Lac	$07^h21^m53^s.4$	$+71^d20^m36^s$	0.3	62.20 ± 1.05	1.00 ± 0.15
Mrk 421	3FGLJ1104.4+3812	BL Lac	$11^h04^m273^s$	$+38^d12^m32^s$	0.03	43.65 ± 1.45	1.00 ± 0.08
TON 0599	3FGL J1159.5+2914	BL Lac	$11^h59^m31^s.8$	$+29^d14^m44^s$	0.7247	111.69 ± 0.88	1.30 ± 0.15
ON +325	3FGL J1217.8+3007	BL Lac	$12^h17^m52^s.1$	$+30^d07^m01^s$	0.131	43.78 ± 4.60	0.80 ± 0.14
W Comae	3FGL J1221.4+2814	BL Lac	$12^h21^m31^s.7$	$+28^d13^m59^s$	0.102	24.70 ± 8.87	1.10 ± 0.09
4C +21.35	3FGLJ1224.9+2122	FSRQ	$12^h24^m54^s.4$	$+21^d22^m46^s$	0.432	114.91 ± 0.59	1.10 ± 0.12
3C 273	3FGL J1229.1+0202	FSRQ	$12^h29^m06^s.6997$	$+02^d03^m08^s.598$	0.158	94.66 ± 0.98	1.20 ± 0.17
3C 279	3FGL J1256.1-0547	FSRQ	$12^h56^m11^s.1665$	$-05^d47^m21^s.523$	0.536	104.29 ± 0.46	1.10 ± 0.16
PKS 1424−418	3FGLJ1427.9-4206	FSRQ	$14^h27^m56^s.3$	$-42^d06^m19^s$	1.522	70.44 ± 0.69	1.5 ± 0.13
PKS 1502+106	3FGLJ1504.4+1029	FSRQ	$15^h04^m25^s.0$	$+10^d29^m39^s$	1.84	90.11 ± 0.70	1.3 ± 0.10
4C+38.41	3FGL J1635.2+3809	FSRQ	$16^h35^m15^s.5$	$+38^d08^m04^s$	1.813	92.99 ± 0.72	1.2 ± 0.15
Mrk 501	3FGL J1653.9+3945	BL Lac	$16^h53^m52^s.2167$	$+39^d45^m36^s.609$	0.0334	33.47 ± 3.76	1.10 ± 10
1ES 1959+65	3FGL J2000.0+6509	BL Lac	$19^h59^m59^s.8521$	$+65^d08^m54^s.652$	0.048	49.55 ± 2.84	1.10 ± 0.14
PKS 2155−304	3FGL J2158.8-3013	BL Lac	$21^h58^m52^s.0651$	$-30^d13^m32^s.118$	0.116	45.93 ± 2.02	0.90 ± 0.20
BL Lac	3FGL J2202.7+4217	BL Lac	$22^h02^m43^s.3$	$+42^d16^m40^s$	0.068	64.10 ± 1.05	1.0±0.10
CTA 102	3FGL J2232.5+1143	FSRQ	$22^h32^m36^s.4$	$+11^d43^m51^s$	1.037	117.42 ± 0.37	1.20 ± 0.19
3C 454.3	3FGL J2254.0+1608	FSRQ	$22^h53^m57^s.7$	$+16^d08^m54^s$	0.859	81.30 ± 0.30	1.30±0.17

Decade-long gamma-ray light curves of blazars

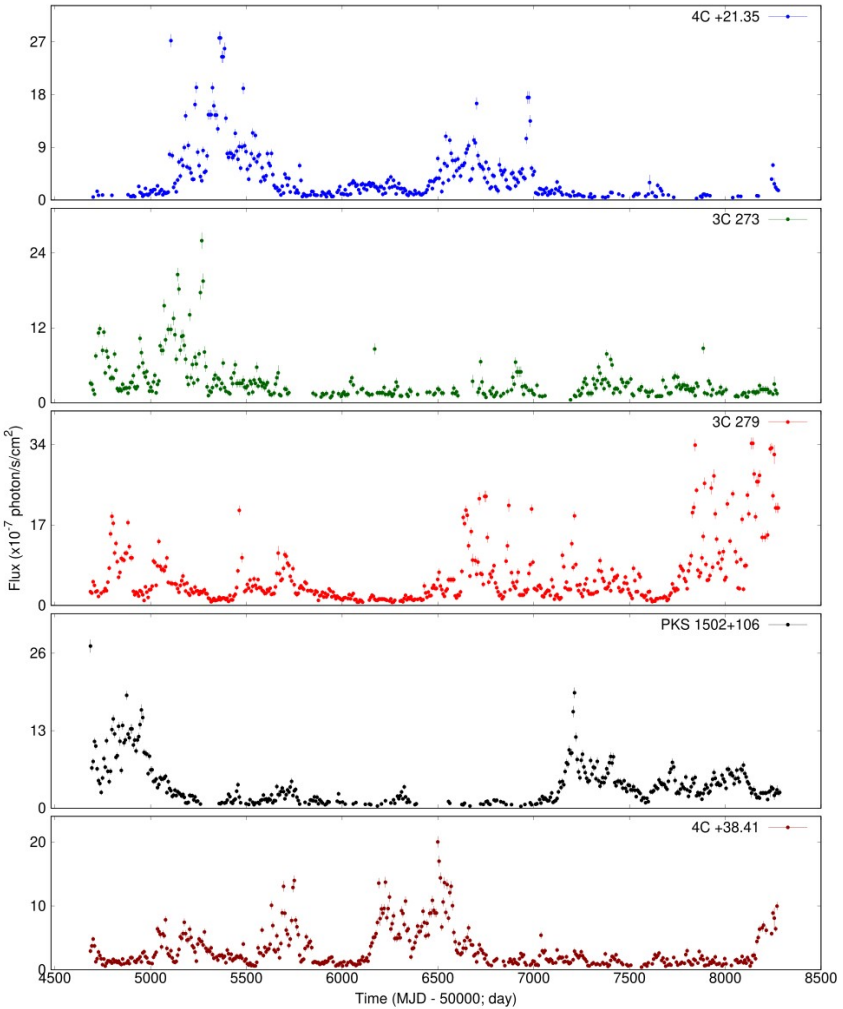

Weekly binned Fermi/LAT observations within the spectral range of 0.1-300 GeV

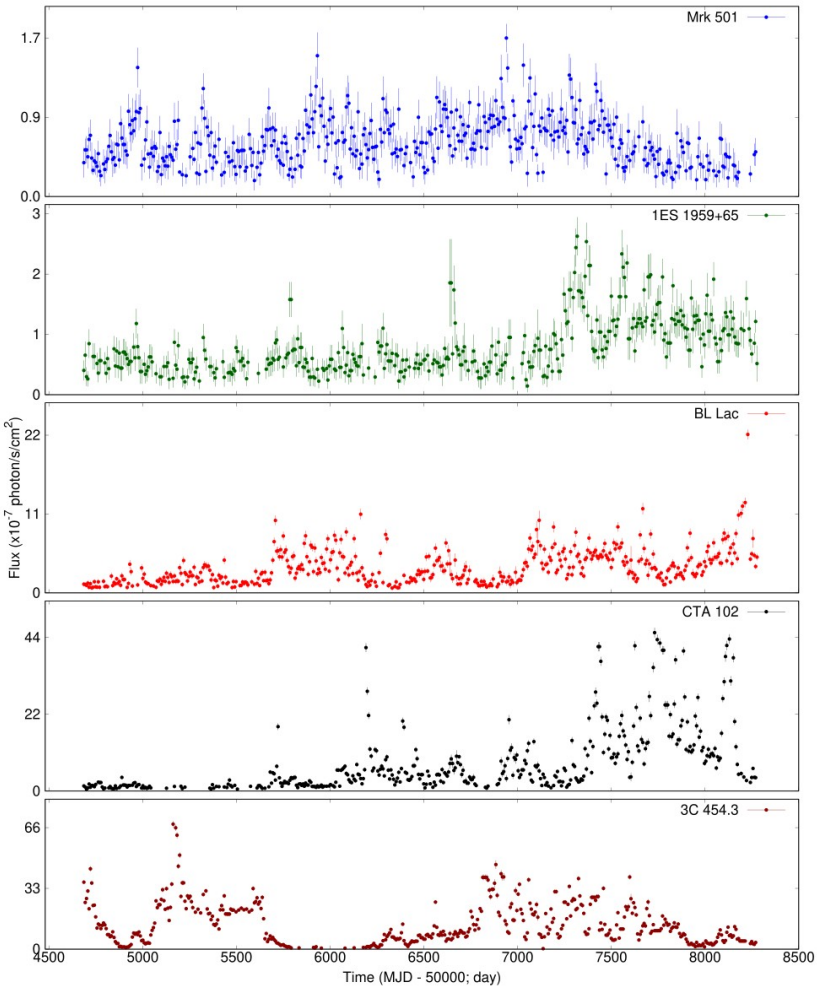

Bhatta & Dhital, 2020, ApJ

Gamma-ray flux distribution

The histogram of the decade-long optical observations were fitted with Gaussian and log-normal PDF

$$f_{\text{normal}}(x) = \exp\left(-\frac{(x-\mu)^2}{2\sigma^2}\right)$$

$$f_{\text{log-normal}}(x) = \frac{1}{xs\sqrt{2\pi}} \exp\left(-\frac{(\ln x - m)^2}{2s^2}\right)$$

In most of the cases, log-normal was found to be a better fit.

Log-normal PDFs could be indication of the fact that the variability phenomena are possibly driven by non-linear and multiplicative processes, rather than stationary and additive processes

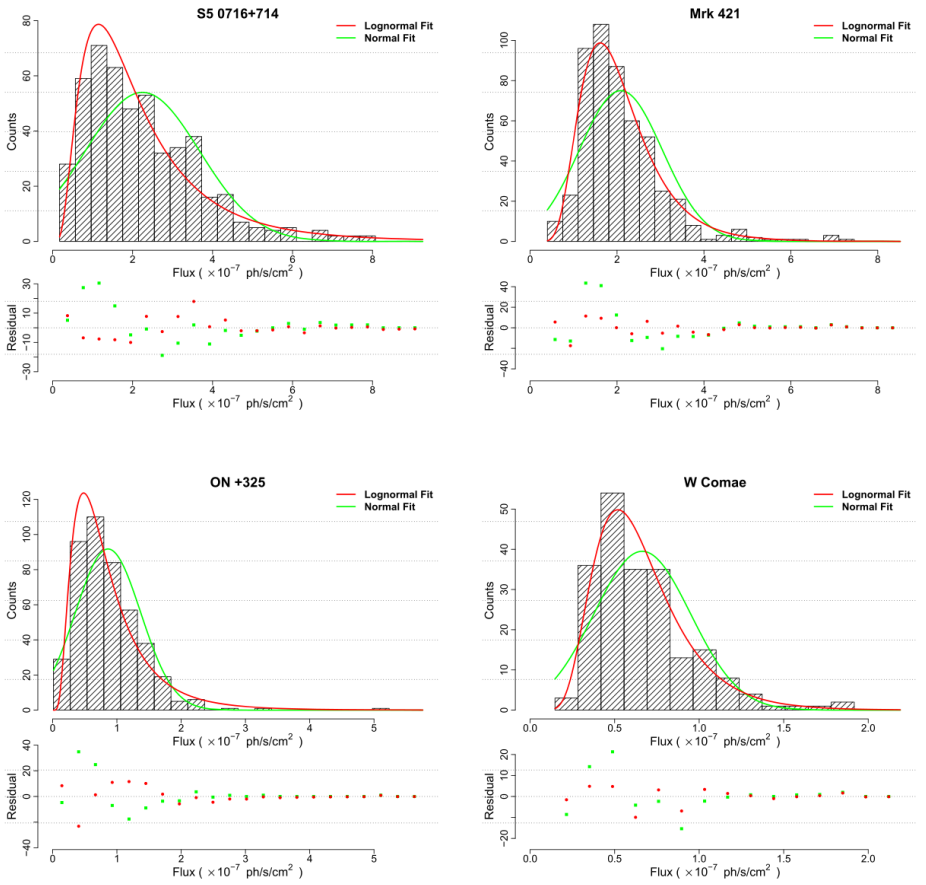

RMS-flux relation in blazars

A linear RMS-flux relation usually indicates a linear correlation between the short-term flux fluctuations to the longer term flux state of an AGN, and the relation is widely found to hold among black hole X-ray binaries.

The RMS is defined as the square-root of the excess variance

$$\sigma_{\rm XS}^2 = S^2 - \langle \sigma_{\rm err}^2 \rangle.$$

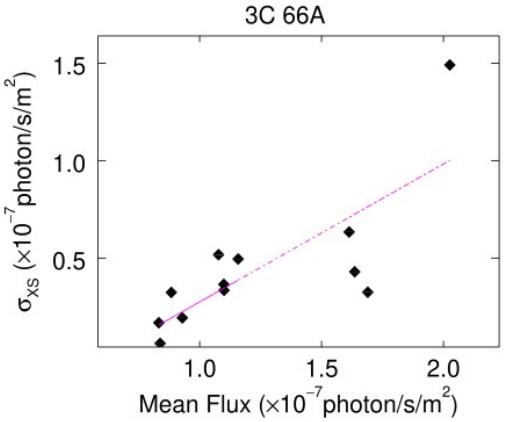

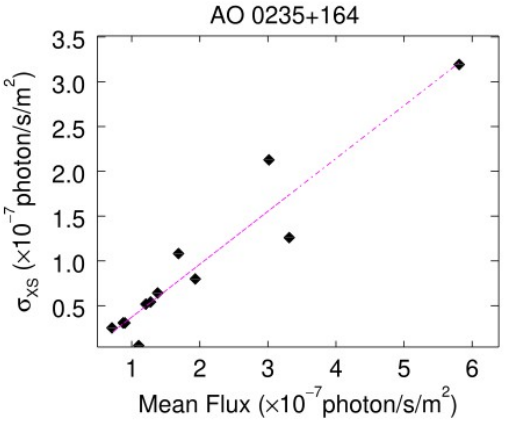

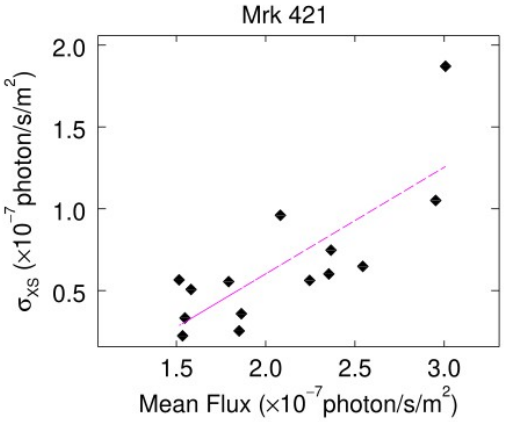

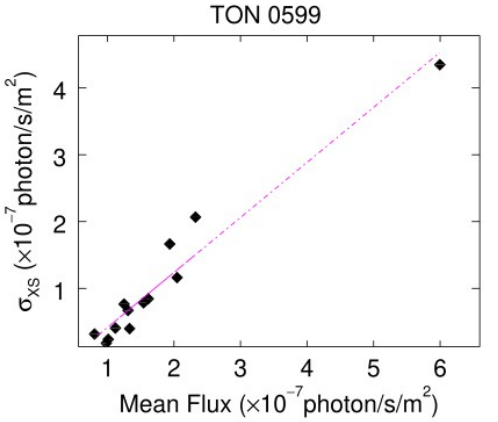

Power spectral density (PSD): Power Spectrum Response method

$$P(\nu) \propto \nu^{-\beta} \qquad \beta \sim 1$$

Source name	Source class	$\beta \pm \Delta\beta$
(1)	(2)	(3)
3C 66A	BL Lac	0.90 ±0.17
AO 0235+164	BL Lac	1.40 ±0.19
PKS 0454-234	BL Lac	1.10 ±0.09
S5 0716+714	BL Lac	1.00 ±0.15
Mrk 421	BL Lac	1.00 ±0.08
TON 0599	BL Lac	1.30 ±0.15
ON +325	BL Lac	0.80 ±0.14
W Comae	BL Lac	1.10 ±0.09
4C +21.35	FSRQ	1.10±0.12
3C 273	FSRQ	1.20±0.17
3C 279	FSRQ	1.10±0.16
PKS 1424-418	FSRQ	1.5±0.13
PKS 1502+106	FSRQ	1.3±0.10
4C+38.41	FSRQ	1.2±0.15
Mrk 501	BL Lac	1.10±10
1ES 1959+65	BL Lac	1.10 ±0.14
PKS 2155-304	BL Lac	0.90±0.20
BL Lac	BL Lac	1.0±0.10
CTA 102	FSRQ	1.20±0.19
3C 454.3	FSRQ	1.30±0.17

Flicker noise or long-memory processes, meaning the short-term disk instabilities may be coupled to the long term changes in the jet emission.

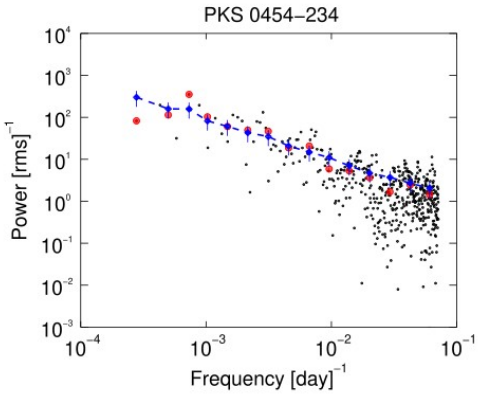

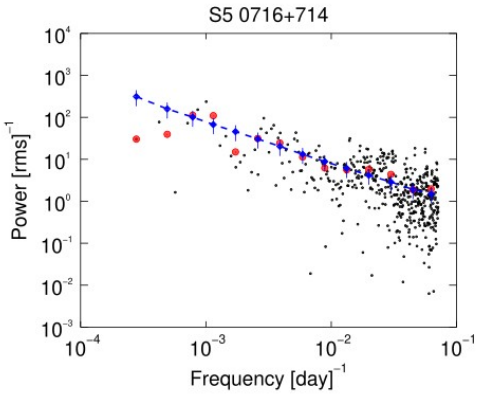

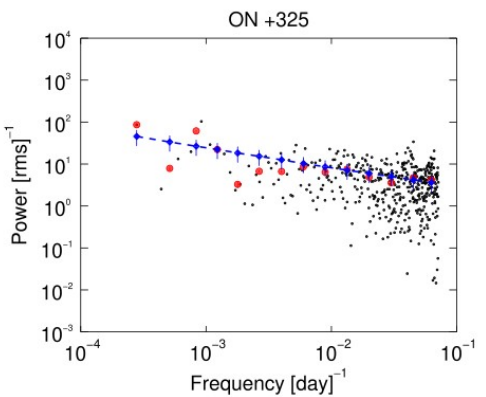

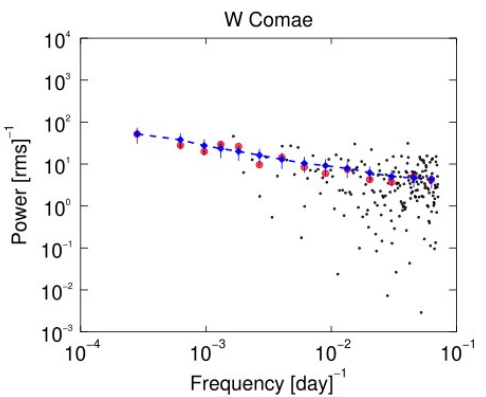

Gamma-ray quasi-periodic oscillations

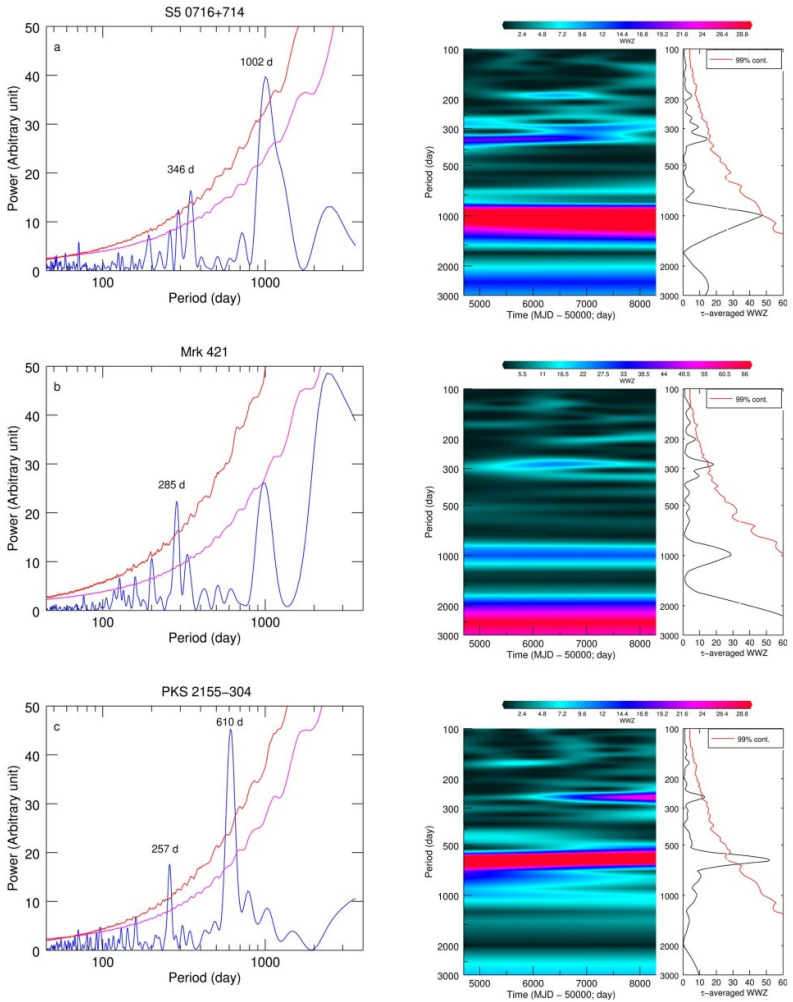

LSP and WWZ studies revealed year timescale QPOs in some of the sources

Bhatta & Dhital 2020, ApJ

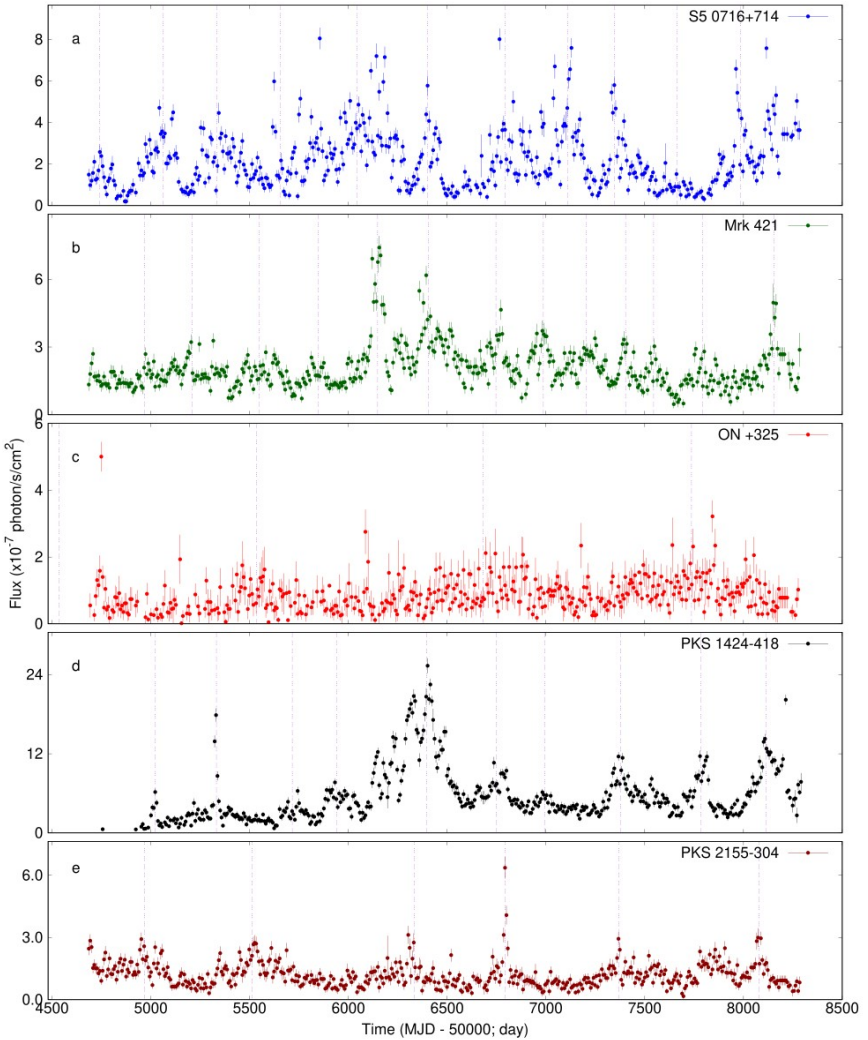

Optical blazar sample sources

Table 1
The Source Sample of the γ-Ray-bright Blazars

Source Name (1)	R.A. (J2000) (2)	Decl. (J2000) (3)	Redshift (4)	Source Class (5)	Mean mag. $\pm$ stdv. (6)	FV (%) (7)
3C 66A	$02^h22^m41^s.6$	$+43^d02^m35^s.5$	0.444	BL Lac	14.69 ± 0.38	37.83 ± 0.23
AO 0235+164	$02^h38^m38^s.9$	$+16^d36^m59^s$	0.94	BL Lac	18.19 ± 0.87	115.00 ± 0.24
S5 0716+714	$07^h21^m53^s.4$	$+71^d20^m36^s$	0.3	BL Lac	13.62 ± 0.59	53.74 ± 0.09
Mrk 421	$11^h04^m273^s$	$+38^d12^m32^s$	0.03	BL Lac	12.96 ± 0.31	29.95 ± 0.15
3C 273	$12^h29^m06^s.6997$	$+02^d03^m08^s.598$	0.158	FSRQ	12.80 ± 0.16	14.44 ± 0.28
3C 279	$12^h56^m11^s.1665$	$-05^d47^m21^s.523$	0.536	FSRQ	15.73 ± 0.82	80.60 ± 0.10
PKS 1424-418	$14^h27^m56^s.3$	$-42^d06^m19^s$	1.522	FSRQ	17.15 ± 1.01	114.24 ± 0.14
Mrk 501	$16^h53^m52^s.2167$	$+39^d45^m36^s.609$	0.0334	BL Lac	13.90 ± 0.07	6.00 ± 1.46
PKS 2155-304	$21^h58^m52^s.0651$	$-30^d13^m32^s.118$	0.116	BL Lac	13.49 ± 0.45	46.01 ± 0.22
BL Lac	$22^h02^m43^s.3$	$+42^d16^m40^s$	0.068	BL Lac	14.44 ± 0.51	46.22 ± 0.07
CTA 102	$22^h32^m36^s.4$	$+11^d43^m51^s$	1.037	FSRQ	16.34 ± 1.02	335.27 ± 0.02
3C 454.3	$22^h53^m57^s.7$	$+16^d08^m54^s$	0.859	FSRQ	15.75 ± 0.63	78.16 ± 0.11

Decade-long optical light curves of blazars

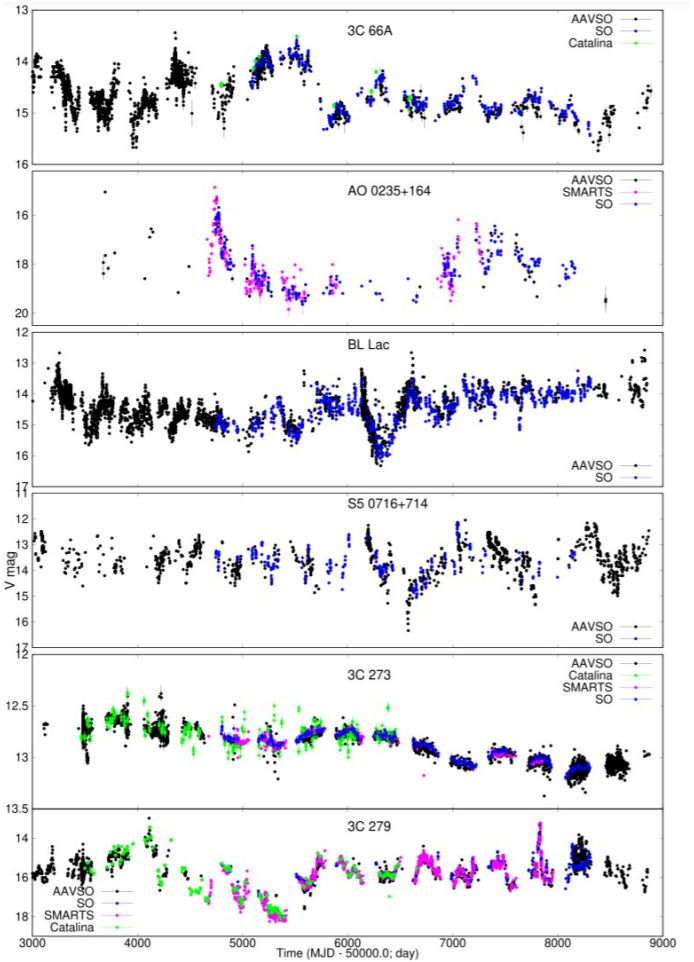

Optical observations from four observatories **AAVSO, Catalina, SMARTS and Steward obs.** were compiled to obtain densely sampled light curves

Bhatta, 2021, ApJ

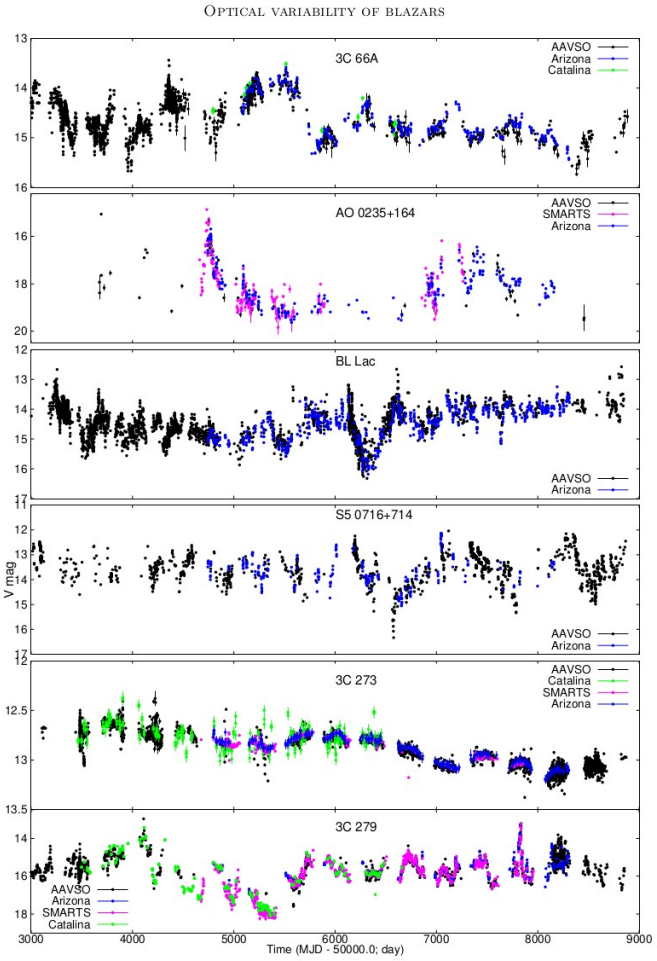

Optical flux distribution

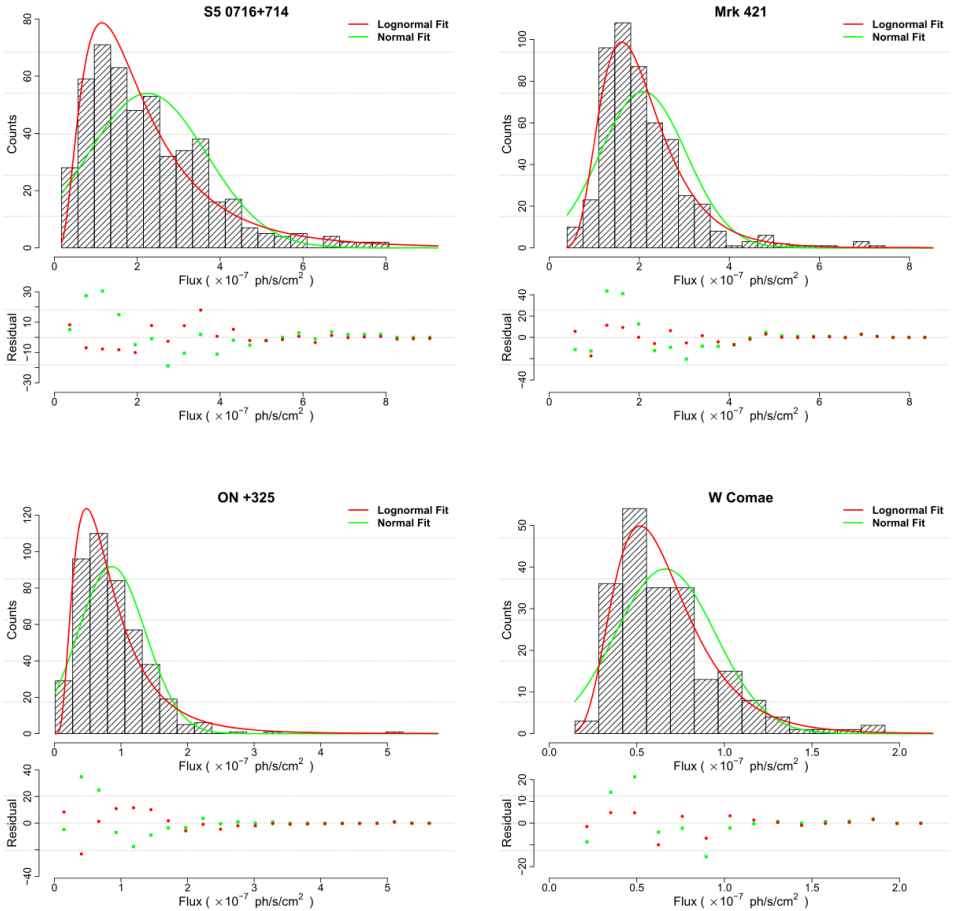

Just like gamma-ray observations, the histogram of the decade-long optical observations were fitted with Gaussian and log-normal PDF

In majority of the cases, log-normal was found to be the best fit

For short-term optical flux distribution see
Pininti, Bhatta et al. 2022, MNRAS

Optical RMS-flux relation

The linear fit was performed in the two cases: a) when the offset parameter fixed to zero and b) when it is free.

As in the gamma-ray band, the optical light curves also showed indication of a linear RMS-flux relation.

A linear RMS-flux relation is often linked with the viscosity driven instability in the accretion disk.

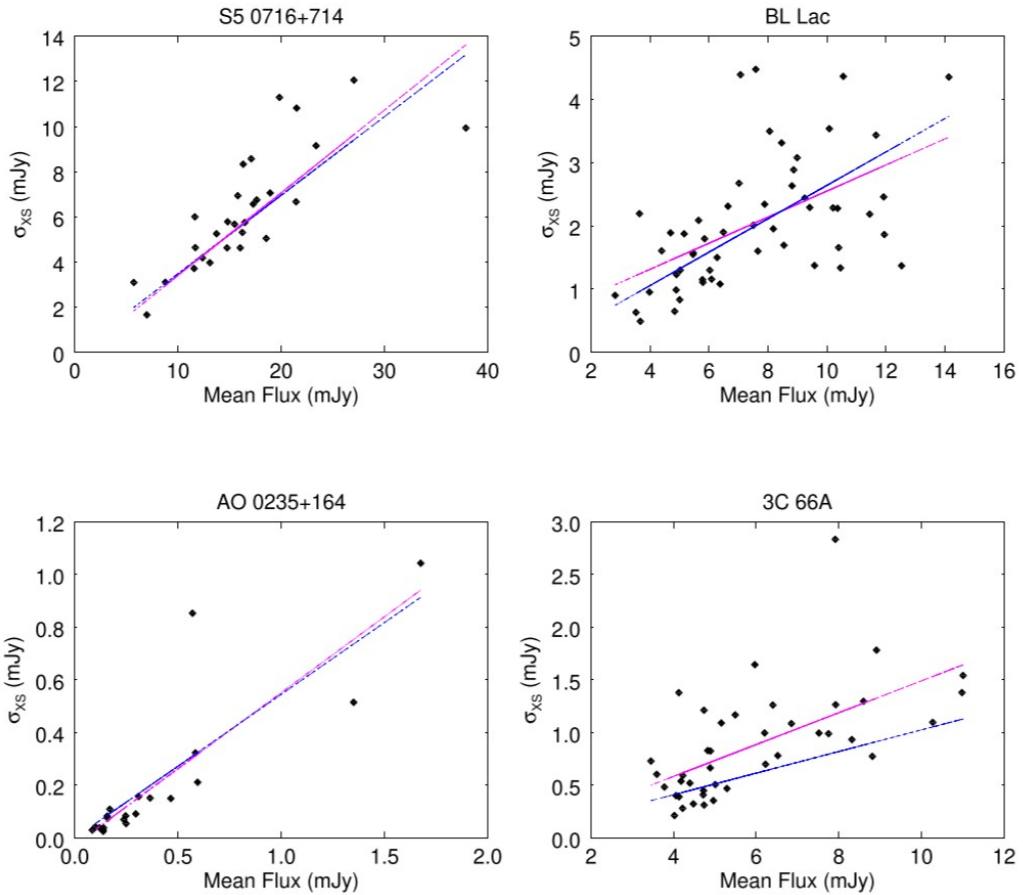

Cross-correlation between optical and gamma-ray observations

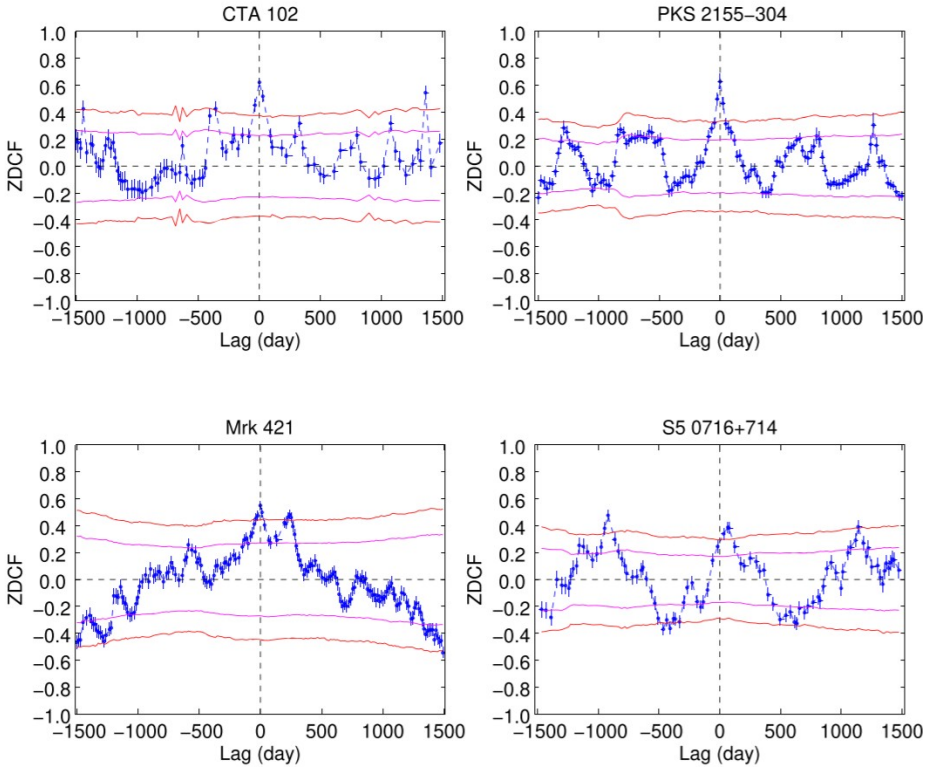

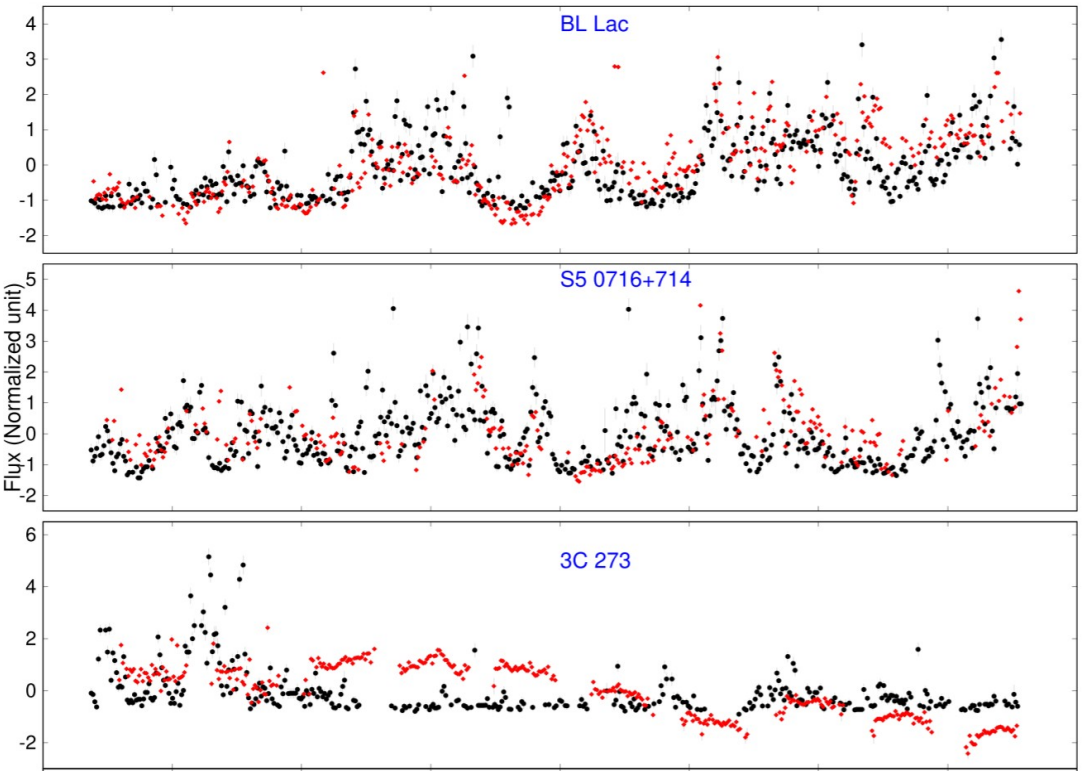

Z-transformed discrete cross-correlation study shows remarkably strong correlation between the optical and gamma-ray emission. However, in the case of the 3C 273 no significant correlation was observed.

Multi-wavelength QPOs

In some of the source, LSP peaks in both the bands were found to coincide in the temporal frequencies.

Because the red-noise nature of the optical and gamma-ray are different, and also the data sampling are not exactly the same, the observed peaks could not have arisen due to some artifact.

MWL QPOs provide important insight into the underlying physics of the central engines.

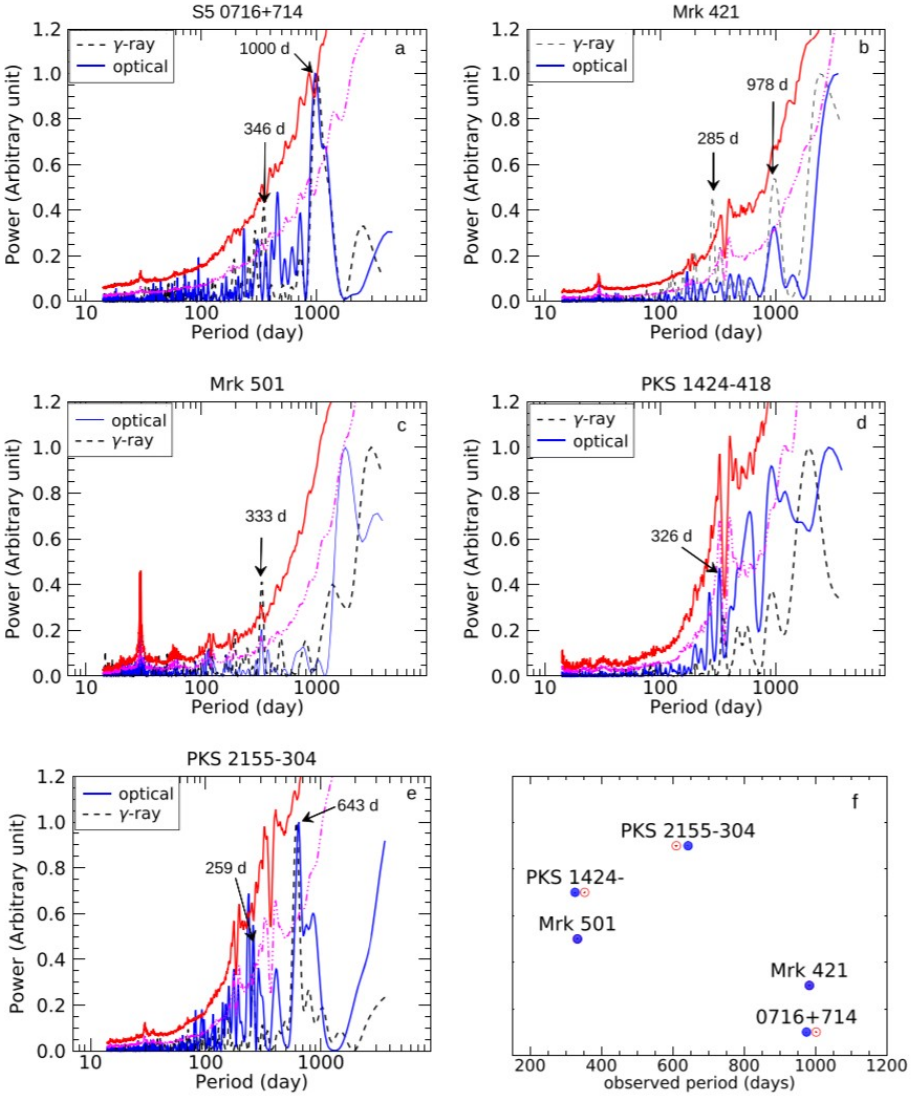

Conclusions

I. Blazars are found to be highly variable in both optical and gamma-ray band, with larger fractional variability in gamma-ray that in the optical.

II. The overall gamma-ray PSD can be fairly approximated by single power-law model with the power-law index nearly unity. Such processes are widely referred as flicker noise and represent long-memory process.

III. Observed RMS-flux relation and lognormal distribution of the flux indicate multiplicative and non-linear nature of the variability processes.

IV. In most of the sources, the correlation between the optical and gamma-ray is strong within a lag/lead of a couple of months. However, it in interesting to note that the correlation does not hold in 3C 273.

V. Year timescale quasi-periodic oscillations were observed both in the optical and the gamma-ray light curves. In the context that not such MWL QPOs are not well-established, these could be important observation. The QPOs can have several explained in various scenario, e.g. binary black holes, Lense-Thirring pression, jet precession and helical magnetic field models.